Rotational diffusion and intermolecular collisions of a spin labeled α-helical peptide determined by electron spin echo spectroscopy

Siobhan M. Miick and Glenn L. Millhauser
Department of Chemistry and Biochemistry, University of California, Santa Cruz, California 95064

ABSTRACT Short peptides that are composed mainly of alanine have recently been shown to form α-helices in aqueous solution at low temperature (Marqusee, S., and R. L. Baldwin. 1987. *Proc. Natl. Acad. Sci.* 84:8898–8902; Marqusee, S., V. H. Robbins, and R. L. Baldwin. 1989. *Proc. Natl. Acad. Sci. USA.* 86:5286–5290). These peptides are excellent models for probing structure and dynamics in isolated helical domains. In previous work we have designed and synthesized spin labeled analogs of these helix-forming peptides and we have shown that these analogs retain the folding characteristics of the parent peptide (Todd, A. P., and G. L. Millhauser. 1991. *Biochemistry.* 30:5515–5523). Using conventional continuous wave electron spin resonance (CW ESR) we have further shown that local motion is more pronounced near the helix amino terminus than in the central region as the peptide is thermally unfolded (Miick, S. M., A. P. Todd, and G. L. Millhauser. 1991. *Biochemistry.* 30:9498–9503). In this present work we use electron spin echo (ESE) spectroscopy to further refine our understanding of the solution dynamics of the 3K-8 peptide, which is a 16-mer with a nitroxide spin label attached at position 8. We find that the spin echo decays are well described by a single exponential function and that the determined correlation times are close to those previously derived from CW experiments. Variable concentration ESE experiments have directly revealed Heisenberg spin exchange (HSE) interactions and we find that the interpeptide collision rate is near to that expected for a free species in solution. This provides strong evidence that the helical conformation of these peptides is not stabilized by intermolecular interactions.

INTRODUCTION

Peptides, which are short linear sequences of amino acids, are emerging as ideal systems for quantitatively testing specific physical aspects of protein stability, structure and dynamics. Using modern design principles, peptides can be synthesized to mimic individual folded domains of complicated multidomain proteins (Marqusee and Baldwin, 1987; Marqusee et al., 1989). This is particularly exciting because these individual domains can now be studied in isolation. Furthermore, these designed peptides are small enough to be simulated with molecular dynamics computer programs (Tirado-Rives and Jorgensen, 1991; Daggett et al., 1991). Thus, the science of small folded peptides exists at an important interdisciplinary interface between protein chemistry, experimental physical chemistry and theoretical molecular dynamics.

Of the various forms of secondary structure in proteins, α-helix is the most common. Approximately forty percent of the residues in solutions proteins exist in α-helical domains. It has recently been shown that 16 residue peptides (16-mers) constructed mainly from the amino acid alanine (Ala) will readily form α-helices in aqueous solution (Marqusee et al., 1989). The high stability of these designed α-helices, relative to their random coil state, was not expected from previous models of the α-helix $\rightarrow$ coil transition. Researchers were surprised by the discovery of these α-helical peptides and presently there is considerable activity looking into the physical foundation of the high helical content. In addition, there is now a flurry of effort aimed at trying to understand the detailed physical properties of short α-helices. Most of this research has used Circular Dichroism (CD) to examine helical stability and Nuclear Magnetic Resonance (NMR) (Bradley et al., 1990; Osterhout et al., 1989) to localize the most helical regions within the folded peptide.

In our research lab we are using spin label electron spin resonance (ESR) to probe the local motions within designed peptides. Whereas the CD and NMR investigations provide information on the thermodynamics and structure, respectively, our experiments reveal the molecular dynamics. Clearly, all three perspectives are needed to develop a complete understanding of folded peptides. Furthermore, we anticipate that our results will serve as an experimental comparison for computer molecular dynamics calculations. To date we have focused on helical peptides. Our approach is to synthesize an analog of a particular peptide sequence that has a spin label site engineered into a specific location (Todd and Millhauser, 1991). Using this approach we have recently reported on the use of conventional continuous wave (CW) ESR to examine the local dynamics in two analogs of the α-helix-forming 3K (I) peptide (Miick et al., 1991). The single letter sequences of these analogs are:

Acetyl—AAACKAAAAKAAAAKA—NH_2 3K-4
Acetyl—AAAAKAACAKAAAAKA—NH_2 3K-8

where A is an Ala (alanine), K is Lys (lysine) and C is Cys (cysteine). The Ala's give the peptide the high helical character and the positively charged Lys residues confer solubility in aqueous solution. These analogs differ from the parent 3K (I) peptide only by a single Ala $\rightarrow$ Cys substitution. Labeling is accomplished with

Address correspondence to Dr. Millhauser.

the methanethiosulfonate spin label (MTSSL) which attaches with 100% specificity to the free —SH on the Cys residue (see below) (Berliner et al., 1982).

The parent 3K (I) peptide exhibits a thermal unfolding transition. At 0°C the fractional helicity is between 70 and 80%, as determined from CD, and the helicity monotonically decreases as the temperature is raised. We showed that our two spin labeled analogs exhibit the same thermal unfolding behavior. Furthermore, the CD signals at 0°C are almost identical to the 3K (I) which quantitatively indicates that the introduction of a 'Cys-MTSSL' residue does not perturb the helical structure of these peptides. We have used CW ESR to determine the rotational correlation time (τ_R) of the nitroxide and we have shown that the measured τ_R is determined by both the global rotational reorientation of the peptide and local motion at the nitroxide attachment point. Thus, by comparing the τ_R's of the two peptides we have been able to track the site specific local dynamics throughout the thermal α-helix → coil transition. At the midpoint of the transition we found that the local motion detected by the label at position 4 is greater than that detected at position 8. This was the first evidence, from the perspective of dynamics, that α-helix unfolding is more pronounced at the helix end (NH_2-terminus) than in the middle. We have also used the denaturant guanidine hydrochloride (Gu · HCl) to compare the thermally unfolded state with the denaturant unfolded state. We have found that only the latter exhibits the position dependant local dynamics theoretically expected for a free chain random coil in solution.

Although our previous studies demonstrate that CW ESR is an extremely powerful method for extracting site specific dynamics in peptides, the information gathered from these ESR experiments is incomplete. Inhomogeneous line broadening, which arises mainly from weak proton hyperfine interactions, obscures the spectral line shapes in motionally narrowed signals ($\tau_R < 2$ ns). To address this, we are now employing electron spin echo (ESE) spectroscopy to directly determine the homogeneous line shape and our experiments on the 3K-8 peptide are the subject of this present work.

Spin echo relaxation measurements directly reveal phase memory decay (i.e., the spin–spin relaxation function), which is the Fourier transform of the homogeneous line shape, for each nitroxide hyperfine line (Gorcester et al., 1989). In turn, the homogeneous line shape provides a high resolution view of spin relaxation processes. If the phase memory decay is purely exponential then the time constant is the spin–spin relaxation time T_2 and the homogeneous linewidth is $1/T_2$. By examining the homogeneous relaxation directly we are able to determine: (*a*) the accuracy of our CW ESR measurements; (*b*) weak Heisenberg Spin Exchange (HSE) effects which are diagnostic for intermolecular collisions, and (*c*) the existence of multiple relaxation components which may indicate the presence of multiple peptide conformations. In this study we have explored both the temperature dependence and the concentration dependence of the phase memory decay for the 3K-8 peptide. We find that our ESE results compare well with our CW ESR results with the latter exhibiting a systematically larger τ_R by ~10%. HSE effects are clearly observed and the determined exchange rate (K_e) falls within the range expected for a diffusion controlled reaction in aqueous solution. This finding is important because it conclusively demonstrates that these short helices are not aggregated and, in turn, their stability arises from intramolecular interactions. Surprisingly, the temperature dependence of K_e does not follow the expected increase with T/η (absolute temperature/viscosity). Finally, at all temperatures and concentrations studied we have found that the phase memory decays are well described by a single exponential function as determined with linear prediction techniques.

ESE OF MOTIONALLY NARROWED NITROXIDE SPECTRA

In the ESE experiments reported here we have used a Hahn two pulse spin echo sequence to directly determine the phase memory decay. The phase memory signal at time τ between the microwave pulses is the height of the spin echo at 2τ which we denote as $S(2\tau)$. Nitroxide spectra, in the motionally narrowed regime, have three nitrogen hyperfine lines ($M = -1, 0, 1$) and if the pulse bandwidth is chosen to completely irradiate a single hyperfine line the phase memory decay of that line is described by

$$S_M(2\tau) \propto [\text{peptide}] \sum_{i=1} \chi_i \exp\{-2\tau/T_{2,i}(M)\}, \quad (1)$$

where [peptide] is the concentration of spin labeled peptide and $T_{2,i}(M)$ is the spin–spin relaxation time for the ith peptide conformation of mole fraction χ_i. If the peptide exists in only one conformation, or there are multiple conformations undergoing rapid interconversion, then the sum in Eq. 1 will contain only one term and $\chi = 1$. Taking into account collisions between peptides the spin–spin relaxation time for the ith conformation is given by the expression

$$T_2^{-1}(M) = A + BM + CM^2 + \tfrac{2}{3}K_e[\text{peptide}], \quad (2)$$

where A, B, and C are the line-shape parameters that arise from rotational reorientation (see below) (Gorcester, et al., 1989), K_e is the second order HSE rate constant. In principle, the three line-shape parameters and K_e may all depend upon the peptide conformation, but for the remainder of this section we consider the behavior of only one term in the sum of Eq. 1 and, for convenience, we suppress expression of the index i. K_e is the rate for spin flips arising from intermolecular collisions and the multiplier of 2/3 statistically corrects for colli-

sions between nitroxides that are in the same hyperfine spin state (Molin et al., 1980). Eq. 2 holds only for the exchange broadened regime where the three hyperfine lines are well resolved and the studies reported here all fall well within this regime. (We point out that the usual expression for T_2^{-1} has the M-independent HSE term absorbed into the A line-shape parameter.)

Of the three line-shape parameters, both B and C are readily determined from CW spectra as well as from ESE phase memory decays. B and C are related to rotational diffusion through the relations (Goldman et al., 1972; Todd and Millhauser, 1991)

$$B = \frac{\pi}{10}\omega_0\left[g^{(0)}D^{(0)}\left(\frac{16}{3}j_0(0) + 4j_0(\omega_0)\right) + 2g^{(2)}D^{(2)}\left(\frac{16}{3}j_2(0) + 4j_2(\omega_0)\right)\right]$$

$$C = \frac{4\pi^2}{5}\left[(D^{(0)})^2\left(\frac{8}{3}j_0(0) - j_0(\omega_a) - \frac{1}{3}j_0(\omega_0)\right) + 2(D^{(2)})^2\left(\frac{8}{3}j_2(0) - j_2(\omega_a) - \frac{1}{3}j_2(\omega_0)\right)\right]. \quad (3a)$$

The spectral densities are

$$j_m(\omega) = \frac{\tau(m)}{1 + \tau(m)^2\omega^2}, \quad (3b)$$

where

$$\tau(0) = 1/(6R_\perp) \quad \tau(2) = 1/(2R_\perp + 4R_\parallel), \quad (3c)$$

and the spherical tensor components are

$$g^{(0)} = (1/\sqrt{6})(2g_{zz} - (g_{xx} + g_{yy})) \quad g^{(2)} = (\tfrac{1}{2})(g_{xx} - g_{yy})$$
$$D^{(0)} = (\tfrac{1}{2}\sqrt{6})(2A_{zz} - (A_{xx} + A_{yy}))$$
$$D^{(2)} = (\tfrac{1}{4})(A_{xx} - A_{yy}). \quad (3d)$$

g_{jj} and A_{jj} are the components of the g-tensor $\mathbf{g}$ and hyperfine tensor $\mathbf{A}$, respectively, ω_0 is the electron Larmor frequency, $\omega_a = (\tfrac{1}{2})a_N$ where a_N is the isotropic hyperfine coupling constant to the nitrogen and $R_\parallel$ and $R_\perp$ are the parallel and perpendicular components of the rotational diffusion tensor. The rotational correlation time is defined as $\tau_R^{-1} = 6(R_\parallel R_\perp)^{1/2}$ and if the motion is isotropic then $\tau(0) = \tau(2) = \tau_R$. In cases where the rotational diffusion is close to isotropic and 100 ps $< \tau_R <$ 1.0 ns then the spectral densities simplify to $j_m(\omega_a) \approx \tau(m)$ and $j_m(\omega_0) \approx 0$ to within an error of less than 3% in B or C. With this simplification the expressions for B and C become linear in $\tau(m)$ and the ratio of $|C/B|$ becomes independent of τ_R and depends only on $N = R_\parallel/R_\perp$.

Experimental values for B and C are determined from ESE spectroscopy using the relations

$$B_{ESE} = \tfrac{1}{2}\{T_2^{-1}(1) - T_2^{-1}(-1)\}$$
$$C_{ESE} = \tfrac{1}{2}\{T_2^{-1}(1) + T_2^{-1}(-1) - 2T_2^{-1}(0)\}, \quad (4a)$$

whereas B and C from CW spectroscopy are determined from

$$B_{CW} = \frac{\sqrt{3}}{4}\Delta H(0)\left\{\sqrt{\frac{V(0)}{V(+1)}} - \sqrt{\frac{V(0)}{V(-1)}}\right\}$$
$$C_{CW} = \frac{\sqrt{3}}{4}\Delta H(0)\left\{\sqrt{\frac{V(0)}{V(+1)}} + \sqrt{\frac{V(0)}{V(-1)}} - 2\right\} \quad (4b)$$

where $V(M)$ is the peak-to-peak height of the Mth hyperfine line in the first derivative CW spectrum and $\Delta H(0)$ is the peak-to-peak width of the $M = 0$ line (Hwang et al., 1975). Because of inhomogeneous broadening of the CW spectra due to proton hyperfine couplings, B_{CW} and C_{CW} are systematically 10–20% larger than their true values. Bales has developed a procedure to correct for this and we have employed his procedure in our previous work and we continue to do so in this present study (Bales, 1989).

EXPERIMENTAL

Peptide spin labeling and purification

The 3K-8 peptide was custom synthesized by the American Peptide Co. (Santa Clara, CA). Methanethiosulfonate spin label (MTSSL) was obtained from Reanal (Budapest, Hungary). Peptides were labeled with MTSSL according to the following reaction.

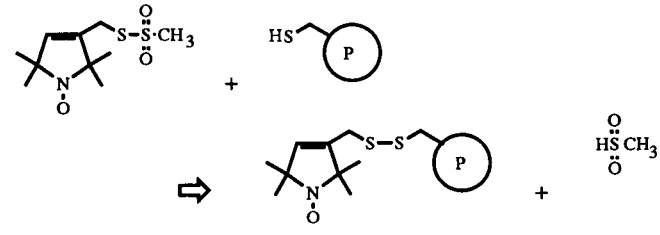

Purification and characterization have been previously described (Todd and Millhauser, 1991). All ESE experiments were performed with buffer conditions of 5 mM MOPS (3-[*N*-Morpholino]propanesulfonic acid) at pH 7. Concentrations for ESE measurements were determined from double integration of the ESR spectrum followed by comparison with a standard aqueous 1.0 mM 4-hydroxy-TEMPO solution. Concentrations determined in this manner are accurate to better than 5%. Following variable temperature ESE, samples were checked for any degradation by HPLC.

Electron spin echo spectroscopy

ESE phase memory decays were acquired with a Bruker ESP 380 spectrometer fitted with a Bruker dielectric resonator and variable temperature accessory. Great care was taken to optimize the ESE signal and we found empirically that a 2-mm inner diameter ESR sample tube containing 20 μL of peptide solution gave the best results. This particular sample geometry contained sufficient spin concentration to give a strong ESE signal without introducing too much dielectric loss from the aqueous solution. The small amount of dielectric loss that did arise was actually beneficial in reducing cavity ringing. For the Hahn ESE sequence we used two equivalent pulses with lengths of 24 ns. We reduced the homogeneity of the static magnetic field to eliminate the free induction decay (FID) and an off-resonance baseline signal was subtracted from each ESE decay. Spectrometer dead time (τ_d) is de-

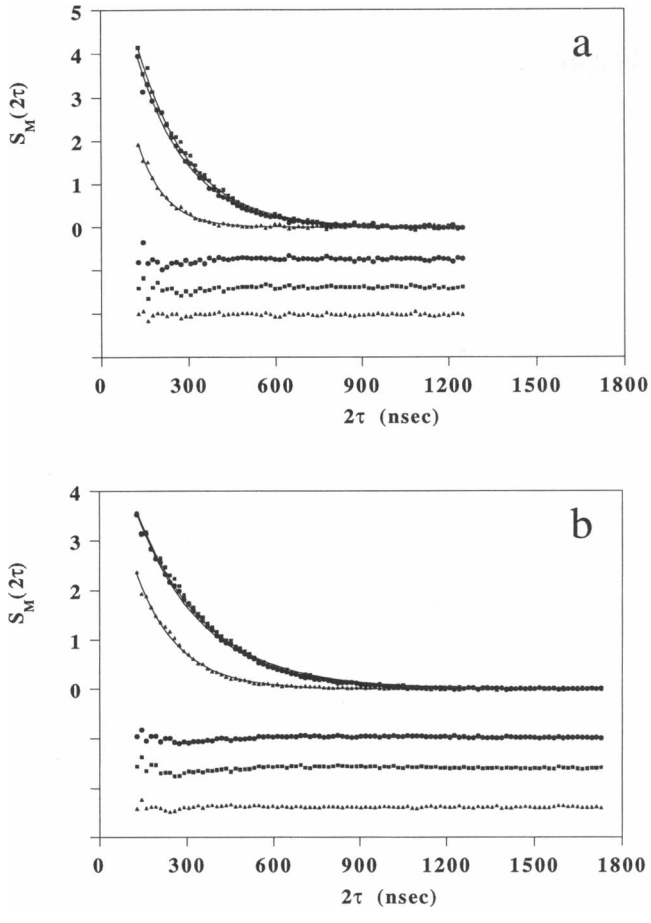

FIGURE 1 ESE phase memory decays for 2.6 mM spin labeled 3K-8 at two temperatures: *a* shows data at 305K and *b* shows data at 325 K. The spin echo data were collected at three field positions corresponding to the three nitroxide hyperfine lines, where (●) is the low field line ($M = 1$), (■) is the middle field line ($M = 0$), and (▲) is the high field line ($M = -1$). Each of the decays were fitted with HSVD analysis and the fit is shown as a solid line. Below each of the decays is the residual for each fit, using the respective symbols.

fined here as the minimum delay between the beginning of the first pulse to the beginning of the second pulse. Under ideal conditions a spectrometer dead time of 56 ns could be achieved, however, in this study we routinely used 64 ns. Data were always collected out to a value of 2τ which was greater than 4–5 times T_2.

ESE phase memory decays were routinely analyzed with a nonlinear-least-squares fitting procedure. For the determination of multiple exponential components we used Hankel singular value decomposition (HSVD) which is a linear prediction technique (Millhauser et al., 1989; Barkhuijsen et al., 1987). The number of exponentials was equated to the number of nonzero singular values.

For the determination of correlation times values we used the following values for the magnetic tensors: $g_{xx} = 2.0086$, $g_{yy} = 2.0066$, $g_{zz} = 2.0032$, $A_{xx} = A_{yy} = 6.23$ *G* and $A_{zz} = 35.7$ *G* (Todd and Millhauser, 1991).

RESULTS

ESE data were collected for all three hyperfine lines of the labeled 3K-8 peptide from 300–334 K. Over this temperature range the fractional helicity changes by approximately a factor of two. In Fig. 1 we show ESE data collected from a 2.6 mM sample at two representative temperatures: 305 and 325 K. The solid lines are the HSVD fits. At both temperatures the $S_M(2\tau)$ signals for high field $M = -1$ line decays much more rapidly than the $M = 0$ and $+1$ lines. This is consistent with the CW spectra where the high field line is broader than the other two lines for these labeled peptides.

HSVD analysis of all of the phase memory decays reveals only a single signal-related singular value for all three hyperfine lines at all temperatures and concentrations studied. We found no exceptions to this behavior. This rigorously demonstrates that the phase memory decays follow a single exponential function under the conditions studied. The high quality of the HSVD fits are apparent in Fig. 1 and residuals show that the random error in the $S_M(2\tau)$ signals is approximately 2–4%. The additional scatter in the residuals for $2\tau < 300$ ns arose from FID created by the second pulse and did not interfere with the HSVD analysis. We will further discuss the temperature dependence of $T_2(M)$ below.

In addition to temperature variation, we also explored $T_2(M)$ at five concentrations and four temperatures in order to reveal HSE interactions of the 3K-8 peptide. The data are shown in Fig. 2 as a plot of $T_2(M)^{-1}$ vs [peptide]. According to Eq. 2 such plots should be linear with slopes independent of M and intercepts that give $T_2(M)^{-1}$ in the limit of infinite dilution. The solid lines are the least-squares fit to a linear function. Within experimental error the linear fits do show uniform slopes among the three hyperfine lines at each temperature. Of all the curves in Fig. 2, the $M = -1$ line at $T = 305$ shows the greatest scatter. However, it should be noted that T_2 for this line is ~70 ns at the higher concentrations and this probably represents the shortest T_2 that can be reliably resolved by ESE for motionally narrowed spectra at this time. We have extracted K_e for each temperature by averaging the slopes for each hyperfine line at that temperature. The results, plotted against T/η, are shown in Fig. 3. To within experimental error, as determined by variations in the slopes, K_e appears to be independent of T.

We now turn to a comparison of these ESE experiments on the 3K-8 peptide to our CW data which we reported previously. Such a comparison is facilitated by gathering ESE data at a concentration that gives the best signal to noise for the spin echo signal $S_M(2\tau)$. From examination of Eqs. 1 and 2, one can see that increasing concentration causes competing effects in the signal strength of $S_M(2\tau)$. As [peptide] is increased $S_M(0)$ increases linearly, however, from HSE effects $T_2(M)$ decreases. Thus, the earliest detectable signal $S_M(2\tau_d)$ has a nonlinear dependence upon [peptide] which reaches a maximum at intermediate concentrations. Inserting Eq. 2 into Eq. 1 and using differential calculus to solve for the maximum of $S_M(2\tau_d)$ as a function of [peptide] one derives the relation

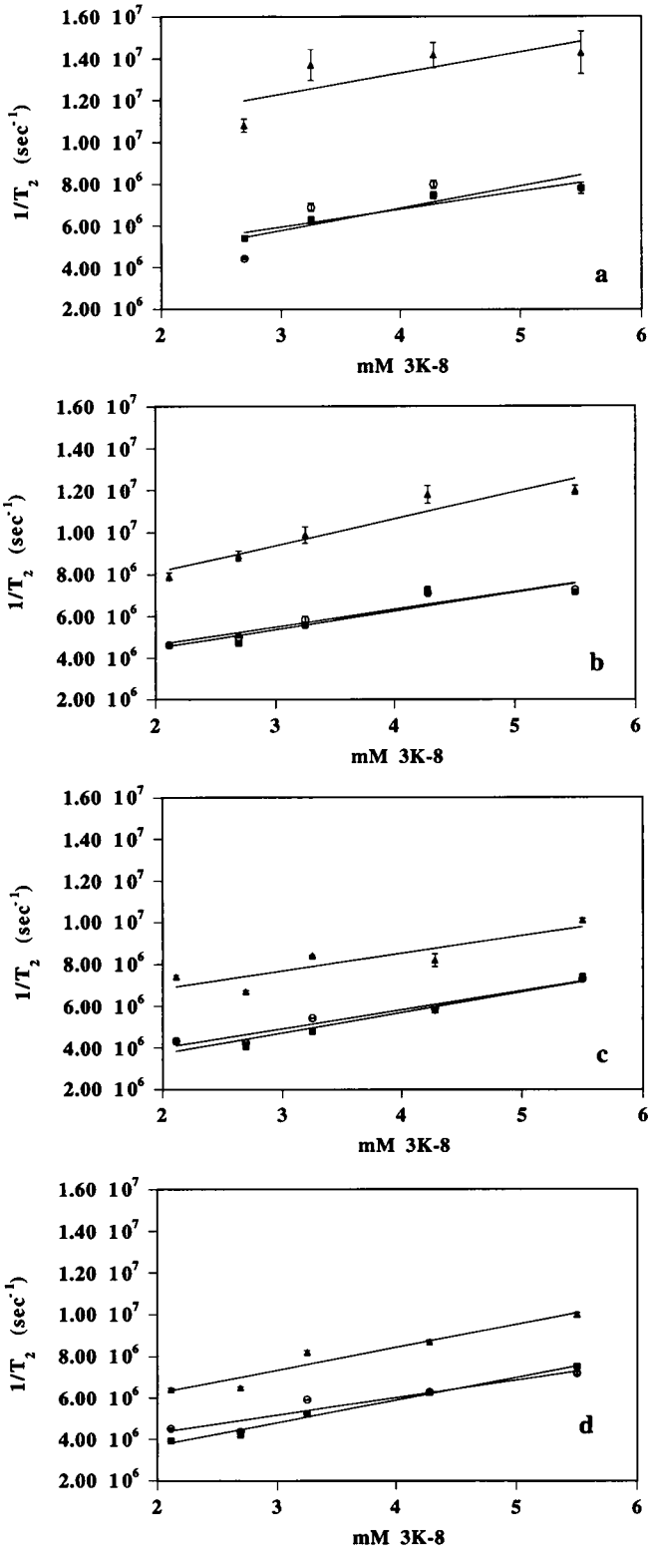

FIGURE 2 $T_2^{-1}(M)$ versus [peptide] data were collected at four temperatures to study the HSE effects for the spin labeled 3K-8 peptide. The $T_2^{-1}(M)$ for each hyperfine line are given by the symbols (●) for the $M = 1$ line, (■) for the $M = 0$ line, and (▲) for the $M = -1$ line. The K_e's were determined from a least squares fit for a linear function for each decay at each field position. The linear fits following Eq. 2 for each concentration series hyperfine line are shown as a solid line. *a* shows data for 305 K, *b* for 315 K, *c* for 325 K, and *d* for 334 K.

$$[\text{peptide}]_{\max} = \frac{3}{4K_e\tau_d}, \tag{5}$$

where $[\text{peptide}]_{\max}$ refers to the concentration of peptide that maximizes the spin echo signal at $2\tau_d$. Using $K_e = 1.5 \times 10^9$ L mol^{-1}s^{-1}, from Fig. 2, and $\tau_d = 64$ ns we calculate $[\text{peptide}]_{\max}$ to be ~4 mM. Eq. 5 is a useful relation but it serves as mainly a starting point for determining the optimum signal. Empirically, we have determined that the most well resolved signal, for a range of τ values, is when [peptide] is between 2 and 3 mM. Thus, for a detailed comparison of CW and ESE variable temperature experiments, we have collected ESE data in 5 K intervals with [peptide] = 2.6 mM (such as the data shown in Fig. 1).

As discussed above and in previous work (Todd and Millhauser, 1991), $C/|B|$ is instrumental in revealing N and the best way to examine this ratio is with a plot of C vs $|B|$. In Fig. 4 we show results from both CW and ESE experiments. Clearly both sets of data are in agreement with the CW data giving a slope of 1.15 and the ESE data giving a slope of 1.12 as determined from linear regression. In previous work we found that MTSSL labeled glutathione also gave $C/|B| = 1.12$. For isotropic motion we expect a value of 1.24 from the magnetic tensor values used here. The difference between this expected value and the experimental value may indicate a small degree of motional anisotropy, however, because there is some uncertainty in the magnetic tensor, values, this assignment is extremely tentative. Furthermore, given the agreement of the $C/|B|$ values between glutathione and the 3K-8 peptide we believe that $C/|B|$ in the range of 1.12 most likely indicates nearly isotropic rotational diffusion.

Using the assignment of isotropic motion either B or C can be used to determine τ_R. Given that there may be systematic errors in the A tensor **A**, we believe that using the B line-shape parameter is preferred for the following reason. C depends upon the square of the spherical tensor terms derived from **A** so that errors in this tensor will cause large systematic errors in τ_R. In contrast, **g** is accurately known and B depends upon the bilinear products of the spherical tensors derived from **g** and **A**. Thus, errors in **A** will impact B in a linear fashion whereas the same errors will impact C quadratically.

From our ESE data B can determined two ways. First, using the same data set shown in Fig. 4 we can directly determine τ_R from B using Eq. 3*a*. These values for B should be independent of [peptide] as predicted by Eqs. 2 and 4. However, it is also instructive to directly test for this independence. Thus, the second way to determine B is to use the values for $T_2(M)^{-1}$ in the limit of infinite dilution derived from the variable concentration studies in Fig. 2. In Fig. 5 we show τ_R vs η/T over a range of temperatures as determined from CW spectroscopy and from ESE spectroscopy at 2.6 mM. Superimposed on these data are τ_R's determined at the four temperatures (in Fig. 2) in the limit of infinite dilution. These latter

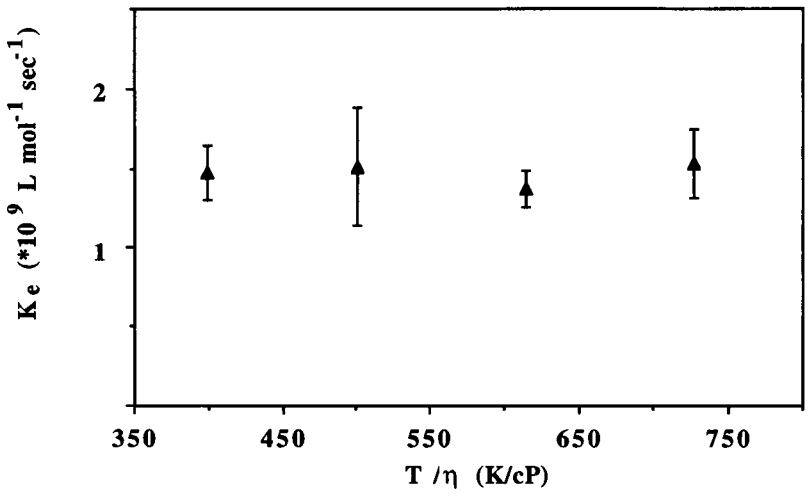

FIGURE 3 K_e, the second order rate constant of spin flips arising from collisions, versus temperature over viscosity (T/η). The K_e's are extracted from the averages of the slopes for each hyperfine line at each temperature (see Fig. 2).

values for τ_R show considerable scatter. However, within experimental error, the τ_R values determined from the two series ESE experiments do not depend upon peptide concentration. Next, turning to a comparison between the CW and ESE data, it can be seen that at high temperature there is excellent agreement in the determination of τ_R. At the two lowest temperatures, however, we find that the CW experiments give a longer τ_R than the ESE experiments by ~15%. We will discuss possible origins of this discrepancy below.

DISCUSSION

The ESE experiments described above have revealed several important details that add considerably to our understanding of the solution dynamics of helical peptides. To appreciate these added details it is important to recognize that CW ESR is limited by inhomogeneous broadening that arises from nitroxide proton hyperfine interactions. Such broadening hides the homogeneous line shape and it is therefore, impossible to determine whether there are multiple peptide species in solution. Thus, a correlation time determined from a CW spectrum may represent an average of several peptide conformations. ESE experiments remove this ambiguity by revealing the Fourier transform of the homogeneous line shape (i.e., the phase memory decay) directly. In the ESE experiments reported here, the decays are well described by a single exponential function and this demonstrates that there is only a single resolved conformational

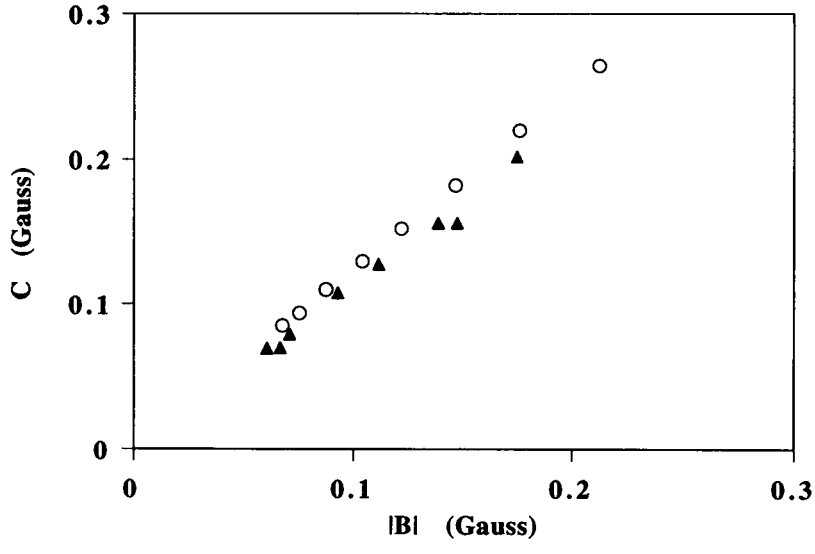

FIGURE 4 C versus $|B|$ in Gauss for the spin labeled 3K-8 peptide. The ESE data shown as (▲) are calculated from Eq. 4*a* and the CW ESR data shown as (○) are calculated from Eq. 4*b*. The similarity of the slopes indicates that N determined from ESE experiments matches N from CW experiments.

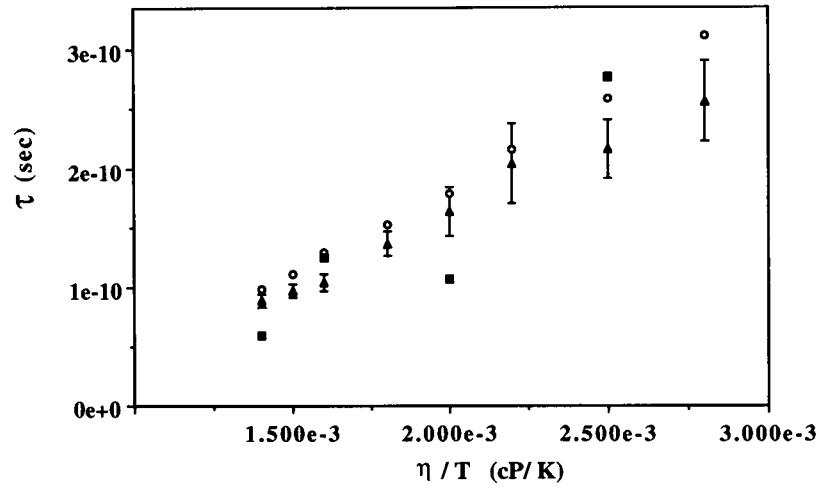

FIGURE 5 Rotational correlation time versus viscosity over temperature (T/η) for the spin labeled 3K-8 peptide. The (○) data is from CW ESR. The (▲) data is from the ESE experiments at 2.6 mM peptide and is plotted with error bars calculated from multiple decays and propagated through the relevant equations. The (■) data is the zero concentration rotational correlation time calculated from the HSE experiments at the y-intercept (see Fig. 2).

species on the ESR time scale. This suggests that correlation times computed from our previous CW studies should match the τ_R's determined from the ESE experiments and indeed this is the case to within 10% throughout most of the temperature range. In addition we have found that the determined correlation times do not depend upon peptide concentration. Thus, we find that our ESE experiments are consistent with our CW ESR experiments which greatly strengthens the conclusions in our previously published work.

Although the CW and ESE data are in general agreement, the lowest temperature data show some inconsistency with the ESE giving a shorter correlation time than that determined from the CW data (see Fig. 5). The origin of this difference is not clear at this time. However, it is possible that several peptide conformations, each with different phase memory times, exist at lower temperatures and that the ESE experiment is sensitive mainly to those conformations with the longest T_2's. In future work we plan to explore this possibility by using T_1 sensitive time domain experiments which spread spin relaxation processes out to longer time scales which, in turn, allow us to probe the lower temperature behavior of our labeled peptides.

Perhaps the most important new contribution of this study is the direct determination of the HSE rate K_e because this parameter provides insight into interpeptide interactions. In examinations of short amphiphilic peptides, unlike the 3K, it was found that the CD signal increased at higher peptide concentrations (Marqusee et al., 1989; Ho and DeGrado, 1987). Thus, the helical state was clearly stabilized by peptide–peptide intermolecular interactions. Similar studies with 3K peptides have shown no such concentration dependence. It has been assumed, therefore, that the helical conformation is monomeric. Nevertheless, to prove that these peptides are monomeric a more direct measure of the peptide–peptide interactions is required. As we have shown, ESE is beautifully suited for this purpose. We have examined the concentration dependence of $T_2(M)$ at four temperatures and we have found that $T_2(M)$ always decreases with increasing concentration for each nitroxide hyperfine line. K_e is readily determined from these data and falls within the range of $1\text{–}2 \times 10^9$ L mol^{-1} s^{-1}. We must now attempt to develop a more quantitative understanding of K_e.

In aqueous solutions the HSE interaction is found to be very efficient and this is referred to as the strong exchange regime (Molin et al., 1980; Nayeem et al., 1989). Each encounter between nitroxides in different hyperfine states results in a 50% chance for a spin exchange event. K_e is therefore related to the second order rate constant for molecular collisions k_d by $K_e = \frac{1}{2}k_d$. k_d is readily calculated from the theory of diffusion controlled reactions. For identical charged species in an ionic medium the expression is

$$k_d = 8\pi N_A D\left[\int_d^\infty \frac{1}{r^2}\exp\left(\frac{z^2 r_0}{r}e^{-r/r_D}\right)dr\right]^{-1}, \qquad (6)$$

where N_A is Avogadro's number, D is the translational diffusion constant for the 3K-8 peptide, z is the number of charges per peptide, r_0 is a characteristic length for electrostatic interactions ($\approx$6.5 Å in H_2O at 320 K), d is the average diameter of the 3K peptide and r_D is the Debye screening length (Steinfeld et al., 1989). (Note that in Steinfeld et al. they have expanded the term $\exp(-r/r_D)$ to first order so their expression in an approximation to Eq. 6.) The effect of large z^2 is to increase the electrostatic repulsion between peptides which, in

turn, decreases k_d. However, if the ionic strength is sufficiently large, then these electrostatic interactions will be screened and this is reflected by a decrease in r_D. In the limit $r_D \rightarrow 0$, the charges on the peptides are completely screened and, using the Stokes-Einsten relation for translational diffusion, Eq. 6 simplifies to the familiar expression for a diffusion controlled rate constant in the absence of electrostatic effects

$$k_{d,0} = \frac{8RT}{3\eta}, \tag{7}$$

where R is the gas constant. Evaluation of Eq. 7 at $T = 320$ gives $k_{d,0} = 1.2 \times 10^{10}$ L mol^{-1} s^{-1} and this is the largest rate constant possible for the collision of species of the same charge. Thus, the expected upper bound for K_e is 6.0×10^9 L mol^{-1} s^{-1}.

Next, we can determine a lower bound for K_e by eliminating the effects of screening and this is done by evaluating Eq. 6 in the limit where $r_D \rightarrow \infty$. Eq. 6 simplifies in this limit and can be solved analytically. Estimating the diameter of the 3K-8 gives $d \approx 25$ Å and using this value we find $k_d = 0.25k_{d,0}$ which gives $K_e = 1.5 \times 10^9$ L^{-1} mol^{-1} s^{-1}. This lower bound agrees very well with our observed values for the 3K-8. It appears, therefore, that the HSE process is diffusion controlled and that there is little screening of the charge on the peptides. This latter point is not surprising because our solutions are at low ionic strength. Nevertheless, it is important to note that even in the absence of screening, charge interactions slow the HSE rate by only a factor of four when compared to the maximum possible rate of 6.0×10^9 L mol^{-1} s^{-1}.

Eq. 7 expresses an important result of the theory of diffusion controlled reactions: if the electrostatic interactions are not too strong, the reaction rate will not depend upon the size of the reacting species. This size independence allows us to compare our findings with HSE studies of simple charged nitroxides in aqueous solution. K_e's for singly charged nitroxides are in the range $0.9–1.9 \times 10^9$ L mol^{-1} s^{-1} (Molin et al., 1980) and K_e increases only slightly for uncharged nitroxides. The values for the 3K-8 also fall within this range and this further supports the hypothesis of a diffusion controlled process.

Bringing together the results of this present work, and our previous work on the 3K-8, we find compelling evidence that these peptides exist as monomeric species in solution. In particular we note that: (*a*) τ_R's are consistent with that expected for a monomeric species, (*b*) τ_R does not depend upon concentration of the peptide, and (*c*) the HSE process arises from a diffusion controlled reaction. It is worthwhile considering how the ESR spectra would be impacted if indeed there were a strong interpeptide attraction leading to aggregation. A careful study on a system that exhibits aggregation has already been performed on a spin labeled version of the peptide melittin (Altenbach and Hubbell, 1988). Melittin is a 26-mer that exists as a monomer in a low salt solution and a tetramer of helices in high salt. In the monomeric form, the ESR spectrum of melittin shows a simple three line motionally-narrowed pattern that is very similar to that observed for the 3K-8. With induction of the tetrameric form, the ESR spectrum changes dramatically and the authors note two main effects. First, the shape of the spectrum indicates a much longer τ_R as expected for a tetramer. Second, the signal intensity decreased significantly due to spin–spin interactions between peptides in the tetramer. In our studies of the 3K-8 we have observed neither of these effects.

In previous work we briefly examined the concentration dependence of the CW spectra and we found that the spectra did not change with increasing concentration. Again, this highlights the increase in sensitivity of ESE to such processes when compared to CW spectroscopy. As before, the CW spectra are less sensitive because of inhomogeneous broadening. Using Eq. 2 we can compute the change in line width due to increased HSE interactions to demonstrate this point. Using $K_e = 1 \times 10^9$ l/mol s and changing the concentration from 1–2 mM results in a change of line width by approximately 40 mG. This difference is very small compared to the peak to peak width of nearly 1.0 G. Thus, ESE is shown to be an excellent technique for revealing HSE interactions at low concentration (i.e., <5 mM labeled peptide).

Finally, we address the temperature dependence of K_e. According to the theory of diffusion controlled reactions, the HSE rate should increase with T/η and such an increase is not observed as shown in Fig. 3. In fact it appears that K_e is nearly independent of temperature. Such behavior has been observed in other systems of free radicals in solutions of low viscosity (Molin et al., 1980). It has been suggested that temperature independence of K_e may signal the onset of weak exchange. We can propose another possibility. As the temperature increases the peptide conformation changes from α-helix to random coil. If the shape of the peptide-label complex is changing then the efficiency of the HSE interaction will also be impacted. Specifically, the random coil state may be more extended than the helical state and many of the collisions between random coils may not bring the nitroxide labels in close enough contact for an exchange event to occur. The result is a weakening of the HSE interaction at higher temperatures which compensates for the increase in collision rate due to greater thermal motion. There may be other possibilities for the independence of K_e with temperature and at this juncture it is very difficult to provide a conclusive mechanism.

CONCLUSIONS

We have demonstrated that ESE spectroscopy provides insight into the solution dynamics of spin labeled peptides beyond that available from CW ESR techniques.

We believe, in fact, that these two techniques are complementary. CW spectroscopy is excellent for the rapid determination of rotational correlation times whereas ESE is beautifully suited for studying the homogeneous line shapes and revealing weak HSE interactions. With the completion of these experiments the stage is now set for using more advanced time domain ESR techniques to reveal the details of peptide dynamics. For example, hydrodynamic calculations have suggested that local correlation functions for peptide dynamics may deviate from exponential behavior. If this is the case then the spectral density of fluctuations will reflect this. By combining ESE experiments with T_1 sensitive pulse sequences we should be able to map the spectral density at three frequencies: 0, ω_a and ω_0 (Gorcester et al., 1989). An exponential correlation function dictates a specific relationship for the spectral density at these three frequencies and so nonexponential relaxation will be readily detectable. In sum, time domain ESR techniques have a very promising future in the experimental study of peptide dynamics.

We thank Professor Ilan Benjamin for his insights on the theory of diffusion controlled reactions. This work was supported by a grant from the National Science Foundation (DMB-8916946). Portions of this work were also supported by faculty research funds granted by the University of California, Santa Cruz. Acknowledgement is made to the donors of The Petroleum Research Fund, administered by the ACS, for partial support of this research (21098-G4).

Received for publication 25 November 1991 and in final form 15 April 1992.

REFERENCES

Altenbach, C., and W. L. Hubbell. 1988. The aggregation state of spin-labeled melittin in solution and bound to phospholipid membranes: evidence that membrane-bound melittin is monomeric. *Proteins.* 3:230–242.

Bales, B. L. 1989. Inhomogeneously broadened spin-label spectra. *In* Biological Magnetic Resonance. Berliner and Reuben, editors. Plenum Publishing Corp., New York. 77–130.

Barkhuijsen, H., R. de Beer, and D. van Ormondt. 1987. Improved algorithm for noniterative time-domain model fitting to exponentially damped magnetic resonance signals. *J. Magn. Reson.* 73:553–557.

Berliner, L. J., J. Grunwald, H. O. Hankovsky, and K. Hideg. 1982. A novel reversible thiol-specific spin-label: papain active site labeling and inhibition. *Anal. Biochem.* 119:450–455.

Bradley, E. K., J. F. Thomason, F. E. Cohen, P. A. Kosen, and I. D. Kuntz. 1990. Studies of synthetic helical peptides using circular dichroism and nuclear magnetic resonance. *J. Mol. Biol.* 215:607–622.

Daggett, V., P. A. Kollman, and I. D. Kuntz. 1991. A molecular dynamics simulation of polyalanine: an analysis of equilibrium motions and helix-coil transitions. *Biopolymers.* 31:285–304.

Goldman, S. A., G. V. Bruno, C. F. Polnaszek, and J. H. Freed. 1972. An ESR study of anisotropic rotational reorientation and slow tumbling in liquid and frozen media. *J. Chem. Phys.* 56:716–735.

Gorcester, J., S. B. Ranavare, and J. H. Freed. 1989. Two-dimensional electron–electron double resonance and electron spin-echo study of solute dynamics in smectics. *J. Chem. Phys.* 90:5764–5786.

Ho, S. P., and W. F. DeGrado. 1987. Design of a 4-helix bundle protein: synthesis of peptides which self-associate into a helical protein. *J. Am. Chem. Soc.* 109:6751–6758.

Hwang, J. S., R. P. Mason, L. Hwang, and J. H. Freed. 1975. Electron spin resonance studies of anisotropic rotational reorientation and slow tumbling in liquid and frozen media. III. Perdeuterated 2,2,6,6-tetramethyl-4-piperidone *N*-oxide and an analysis of fluctuating torques. *J. Phys. Chem.* 79:489–511.

Marqusee, S., and R. L. Baldwin. 1987. Helix stabilization by $Glu^- \cdots Lys^+$ salt bridges in short peptides of de novo design. *Proc. Natl. Acad. Sci. USA.* 84:8898–8902.

Marqusee, S., V. H. Robbins, and R. L. Baldwin. 1989. Unusually stable helix formation in short alanine-based peptides. *Proc. Natl. Acad. Sci. USA.* 86:5286–5290.

Miick, S. M., A. P. Todd, and G. L. Millhauser. 1991. Position-dependent local motions in spin-labeled analogues of a short α-helical peptide determined by electron spin resonance. *Biochemistry.* 30:9498–9503.

Millhauser, G. L., A. A. Carter, D. J. Schneider, J. H. Freed, and R. E. Oswald. 1989. Rapid singular value decomposition for time-domain analysis of magnetic resonance signals by use of the Lanczos algorithm. *J. Magn. Reson.* 82:150–155.

Molin, Y. N., K. M. Salikhov, and K. I. Zamaraev. 1980. Spin Exchange: Principles and Applications in Chemistry and Biology. Springer-Verlag, Berlin.

Nayeem, A., S. B. Rananavare, V. S. S. Sastry, and J. H. Freed. 1989. Heisenberg spin exchange and molecular diffusion in liquid crystals. *J. Chem. Phys.* 91:6887–6905.

Osterhout, J. J., R. L. Baldwin, E. J. York, J. M. Stewart, H. J. Dyson, and P. E. Wright. 1989. ^1H NMR studies of the solution conformations of an analogue of the C-peptide of ribonuclease A. *Biochemistry.* 28:7059–7064.

Steinfeld, J. I., J. S. Francisco, and W. L. Hase. 1989. Chemical Kinetics and Dynamics. Prentice Hall, Inc., New Jersey.

Tirado-Rives, J., and W. L. Jorgensen. 1991. Molecular dynamics simulations of the unfolding of an α-helical analogue of ribonuclease A S-peptide in water. *Biochemistry.* 30:3864–3871.

Todd, A. P., and G. L. Millhauser. 1991. ESR spectra reflect local and global mobility in a short spin-labeled peptide throughout the α-helix $\rightarrow$ coil transition. *Biochemistry.* 30:5515–5523.